

Enhanced Generative Data Augmentation for Semantic Segmentation via Stronger Guidance

Keywords: Data Augmentation, Stable Diffusion, Semantic Segmentation

Abstract: Data augmentation is crucial for pixel-wise annotation tasks like semantic segmentation, where labeling requires significant effort and intensive labor. Traditional methods, involving simple transformations such as rotations and flips, create new images but often lack diversity along key semantic dimensions and fail to alter high-level semantic properties. To address this issue, generative models have emerged as an effective solution for augmenting data by generating synthetic images. Controllable Generative models offer data augmentation methods for semantic segmentation tasks by using prompts and visual references from the original image. However, directly employing these models presents challenges, such as creating an effective prompt and visual reference to generate a synthetic image that accurately reflects the content and structure of the original. In this work, we introduce an effective data augmentation pipeline for semantic segmentation using Controllable Diffusion model. Our proposed method includes efficient prompt generation using *Class-Prompt Appending* and *Visual Prior Blending* to enhance attention to labeled classes in real images, allowing the pipeline to generate a precise number of augmented images while preserving the structure of segmentation-labeled classes. In addition, we implement a *class balancing algorithm* to ensure a balanced training dataset when merging the synthetic and original images. Evaluation on PASCAL VOC datasets, our pipeline demonstrates its effectiveness in generating high-quality synthetic images for semantic segmentation.

1 INTRODUCTION

Semantic segmentation is a fundamental computer vision task that involves classifying each pixel in an image. Deep learning models have significantly advanced semantic segmentation methods. These models are usually trained on large-scale datasets with dense annotations, such as PASCAL VOC (Everingham et al., 2015), MS COCO (Lin et al., 2014), BDD100K (Yu et al., 2020), and ADE20K (Zhou et al., 2019). It is often necessary to re-label the data to address a specific task. However, labeling a new dataset to enable accurate model learning is time-consuming and costly, particularly for semantic segmentation tasks that require pixel-level labeling.

An alternative to enhancing data diversity without annotating a new dataset is data augmentation, which creates more training examples by leveraging an existing dataset. Commonly used data augmentation methods in semantic segmentation include rotating, scaling, flipping, and other manipulations of individual images. These techniques encourage the model to learn more invariant features, thereby improving the robustness of the trained model. However, basic transformations do not produce novel structural elements, textures, or changes in perspective. Consequently, more advanced data augmentation meth-

ods utilize generative models for different tasks, such as those described in the following works (Trabucco et al., 2024; Azizi et al., 2023; He et al., 2023; Fang et al., 2024; Wu et al., 2024). Generative models leverage the ability to create new images based on inputs such as text, semantic maps, and image guidance (edge, line art, soft edge) to specific tasks and data augmentation needs. Notably, Stable Diffusion (SD) (Rombach et al., 2022; Podell et al., 2024) and its variants (Zhang et al., 2023; Mou et al., 2023) excel in producing high-quality images based on input conditions.

The segmentation mask annotation can be easily computed in data augmentation using simple transformations. However, with generative models, data augmentation is more problematic as it requires generating new images while still matching the segmentation mask. A simple approach to the aforementioned challenge is to use Inpainting model (Rombach et al., 2022) to change the labeled classes in the images while preserving the remaining information. Although it can increase the diversity of the data classes, the diversity of the surrounding elements is limited when applying the method above. In addition, some studies (Mou et al., 2023; Zhang et al., 2023; Chae et al., 2023) propose image generation models that can be controlled from the segmentation mask of the

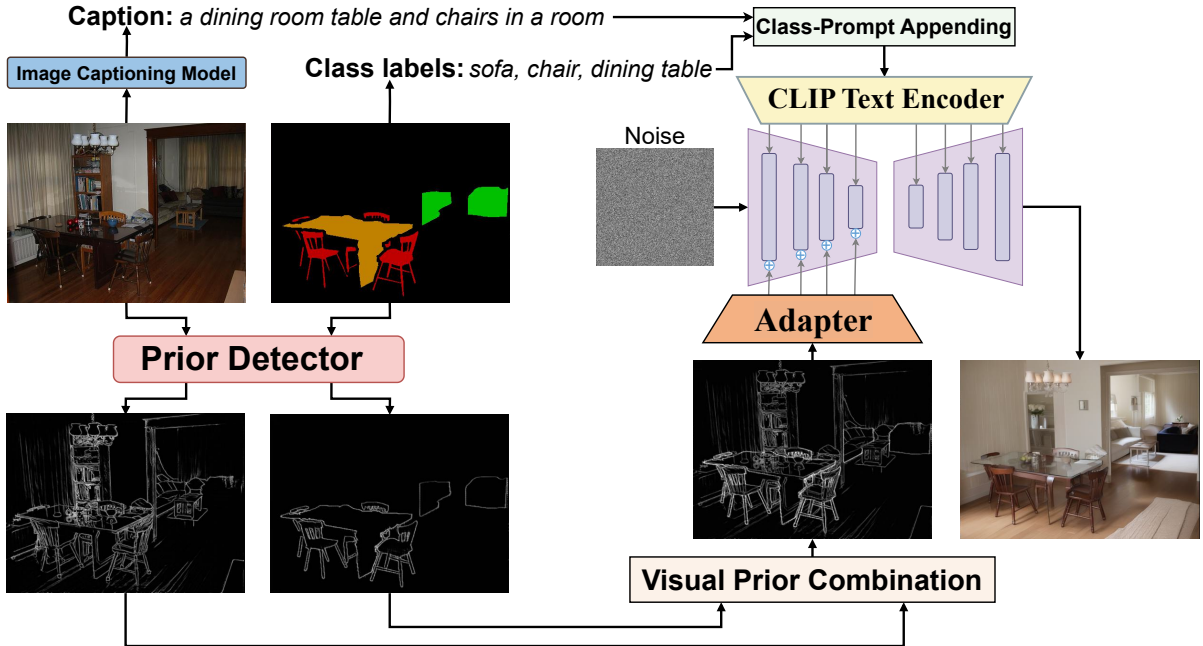


Figure 1: The controllable data augmentation pipeline for the semantic segmentation task combines our proposed methods: Class-Prompt Appending and Visual Prior Blending

image. However, all the above-mentioned methods require training on semantic segmentation datasets for generative models, which results in the model being unable to generate classes that are not part of the training dataset.

With a deep understanding of pre-trained generative models, we can identify their strengths with a vast knowledge base, such as generality and good controllability. In this paper, we propose using Controllable Generative models with prior visual without training on semantic segmentation datasets to augment data for semantic segmentation. The proposed methods ensure that the generated images match the original images in terms of the number of labels and their structures but with transformations in color, context, and style. To achieve high performance in data augmentation, we propose *Visual Prior Blending* and *Class-Prompt Appending* to enhance the visual representation of labeled classes. This combination method is depicted in Figure 1. In addition, we also use a *class balancing algorithm* to control the number of classes during image generation so that when combining the synthetic dataset and the original data, the classes in the extended dataset are more balanced.

2 RELATED WORK

Data augmentation using generative models is commonly applied in classification tasks (Trabucco et al., 2024; Azizi et al., 2023; He et al., 2023). Unlike classification tasks, to augment data for Segmentation or Object Detection tasks, where the synthetic images must ensure the location of the objects, Inpainting model (Rombach et al., 2022) is considered an option because it allows to specify what to edit as a mask. However, because it is only possible to edit objects in the mask, the contexts around the object are almost kept the same, which leads to the synthetic images needing to be more diverse in terms of content.

Some studies (Mou et al., 2023; Zhang et al., 2023; Chae et al., 2023) suggest using semantic segmentation maps to guide image generation. This means labeling each pixel to show which class it belongs to, helping to create accurate images with correct object locations and details. However, these methods require training on segmentation datasets, limiting synthetic images to the trained classes and making them unclear for untrained ones. For example, the method in (Mou et al., 2023; Zhang et al., 2023) is trained on the ADE20K (Zhou et al., 2019) dataset, which has various images from different contexts like indoor, outdoor, industrial, and natural scenes. Consider the task of generating synthetic images for the BDD100K dataset (Yu et al.,

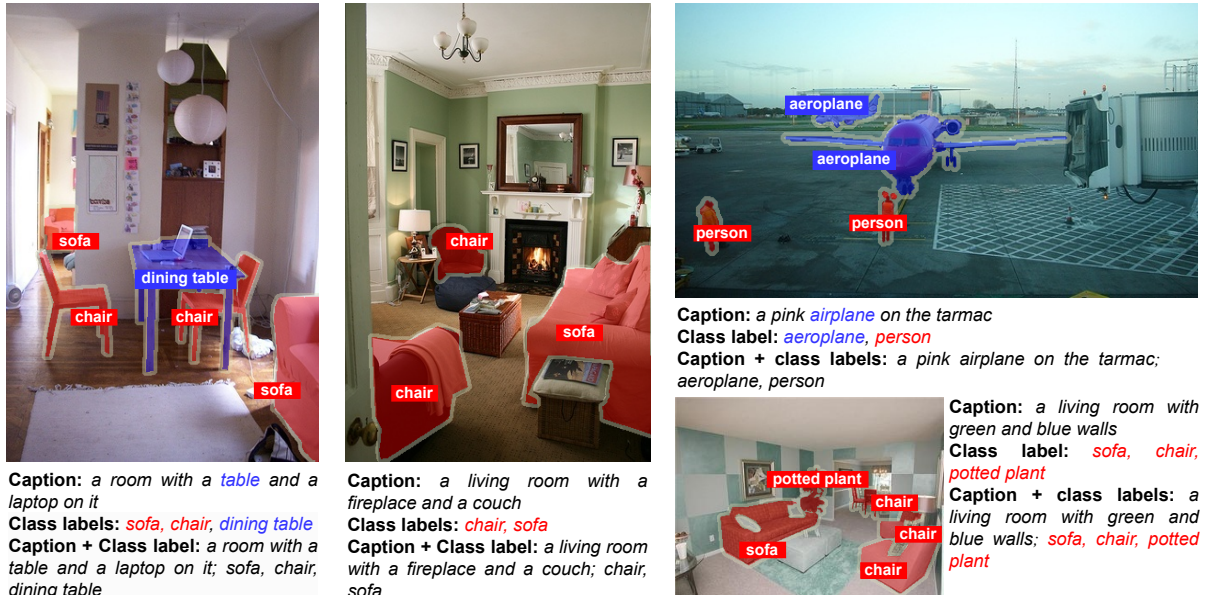


Figure 2: **Classes missing in the generated prompts:** Red describes the missing classes in the generated prompt while blue marks the ones appearing in the sentence.

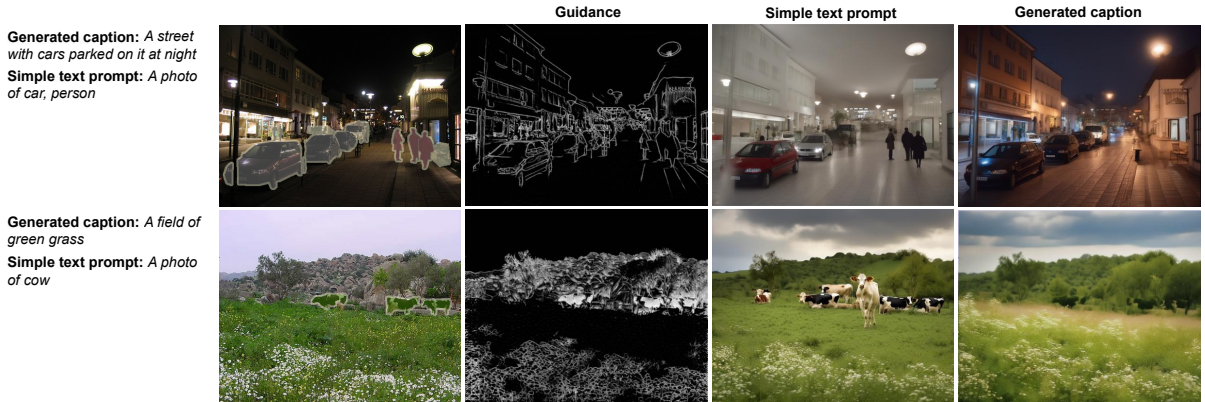
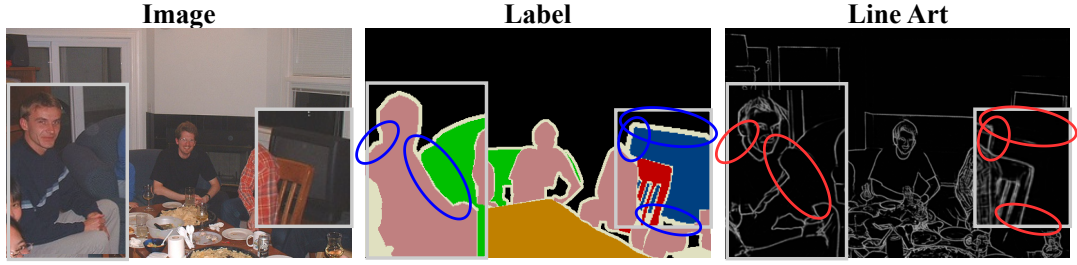


Figure 3: **Common issues of using generated captions and simple text prompts:** In addition to generated prompts and simple text prompts, the four visualizations include: original images with labeled classes, guidance images (line art), images generated by simple text prompts, and images generated by generated prompts.

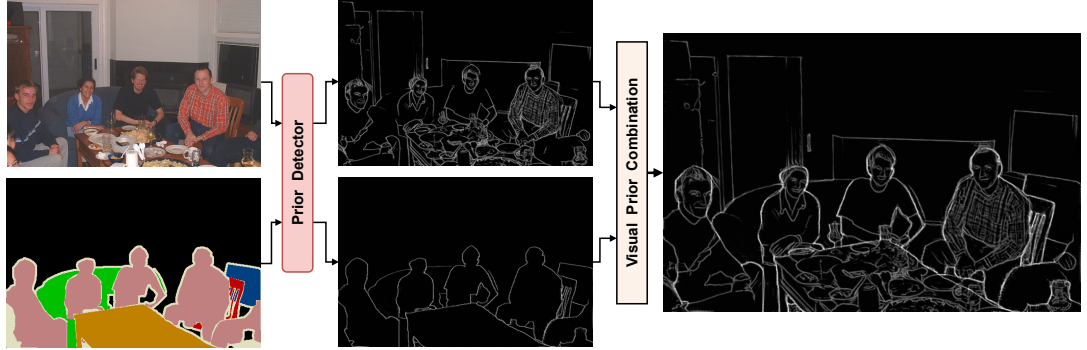
2020), which contains vehicle camera images. The model cannot produce classes absent in the ADE20K dataset, such as traffic signs, traffic lights, and road markings. Due to this limitation, we avoid using models guided by semantic segmentation maps in this study to maintain the generality of our method.

Instead of directly selecting synthetic images to train the model, some studies (Fang et al., 2024; Wu et al., 2024) propose using post-filtering techniques to choose the best synthetic images. However, selecting one high-quality image from many can be time-consuming, and imperfect filtering can lead to a low-quality synthetic dataset. In addition, with the ability to generate different images from the same input

and change the random seeds, selecting the best ones based on multiple results does not accurately reflect the image generation ability. Therefore, in this paper, we directly use the generated images without going through any post-filtering techniques to demonstrate the effectiveness of the proposed method. In addition, in Section 4.3, we also integrate the filter using CLIP Encoder (Fang et al., 2024) to demonstrate the compatibility of the proposed method when applying filters.



(a) An example of information loss occurs when using Line Art Detection, particularly in the reddish areas, where information is lacking.



(b) The results of the Visual Prior Blending method demonstrate that previously edge-deficient objects are now fully detailed, and the edge features of the labeled classes are more prominent compared to the background, thereby enhancing the generative model’s attention capability.

Figure 4: The edge feature results before (a) and after (b) using the Visual Prior Blending method..

3 METHOD

Our proposed image data augmentation pipeline is shown in Figure 1, which consists of three main components: (1) Text prompt construction, (2) Visual Prior Blending, and (3) Controllable Diffusion Generation. *Class-Prompt Appending* append “*class prompt*” including the classes visible in the image with “*caption*” generated from the Image Captioning model. *Visual Prior Blending* method combines the visual pre-information of the real image and the segmentation map. The results of the above two methods are fed into the Controllable Steady Diffusion model to generate the synthetic image. In addition, to generate synthetic data from a given dataset, we use *class balancing algorithm* to generate data with even distribution among classes. Next, we provide a detailed description of each component.

3.1 Preliminary

Diffusion models comprise both forward and reverse processes (Ho et al., 2020). In the forward process, a Markovian chain is defined with noise added to the clean image x_0 :

$$x_t = \sqrt{\bar{\alpha}_t}x_0 + \sqrt{1 - \bar{\alpha}_t}\varepsilon, \quad \varepsilon \sim \mathcal{N}(0, I) \quad (1)$$

where x_t is the noise image at time step t , ε is a noise map sampled from a Gaussian distribution, and $\bar{\alpha}_t$ denotes the corresponding noise level. The neural network ε_t is parameterized by θ , which is optimized to predict the noise added to ε_t in the reverse process. A classical Diffusion model is typically optimized by:

$$\mathcal{L}_{DDPM} = \mathbb{E}_{x_0, t, \varepsilon_t} \|\varepsilon_t - \varepsilon_\theta(x_t, t)\|_2^2 \quad (2)$$

In the context of controllable generation (Zhang et al., 2023; Mou et al., 2023), when given a condition image c_v and a text prompt c_t , the diffusion training loss function at time t can be re-written as:

$$\mathcal{L} = \mathbb{E}_{x_0, c_v, c_t, t, \varepsilon_t} \|\varepsilon_t - \varepsilon_\theta(x_t, t, c_v, c_t)\|_2^2 \quad (3)$$

3.2 Generative Data Augmentation Pipeline

3.2.1 Text prompt construction

To generate an image containing the labeled classes as in the original image, we need a robust prompt

that describes the original image well to serve as input to the SD model. A simple way to do this is by constructing a prompt based on the labeled classes. For example, if image I_i contains target classes $C_i = [c_1, \dots, c_M]$, where M is the number of classes in image I_i , we can construct a simple prompt such as: “ c_1, \dots, c_M ” or “A photo of c_1, \dots, c_M ”. However, using a prompt that only lists target classes may not clearly describe the original image’s layout. To improve this, we can use the existing or generated captions from the training images in these datasets as text prompts for SD. For example, we can use the provided captions when using the COCO dataset (Lin et al., 2014). However, most datasets, such as PASCAL VOC (Everingham et al., 2015), BDD100K (Yu et al., 2020), and ADE20K (Zhou et al., 2019), do not have captions, while annotating captions for images also requires intensive labor. Therefore, we propose using an Image Captioning model such as BLIP-2 (Li et al., 2023) to generate captions for each image. However, image captions have limitations compared to simple prompts, as they often omit some of the actual classes present in the image (as shown in Figure 2). This issue results in missing class names in the captions when using generated descriptions.

Illustrated in Figure 3, some examples demonstrate using simple text prompts and generated captions to create synthetic images through the Controllable SD model. The results indicate that using simple text prompts produces images with messy layouts that do not match the original while using generated prompts leads to missing classes in the generated images due to their absence in the generated captions. However, we observe that these two methods can complement each other’s weaknesses. Therefore, we propose combining generated captions with the image’s class labels to address these limitations. With an image I_i , we append the generated captions \mathcal{P}_i^g with the class labels \mathcal{P}_i^c to generate new text prompts P_i^* . This process, known as *Class-Prompt Appending* (Nguyen et al., 2023), can be represented as: $P_i^* = [\mathcal{P}_i^g; \mathcal{P}_i^c]$. For example, in the sub-figure in the top-right corner of Figure 2, the prompt generated by our proposed method would be “a pink plane on the tarmac; aeroplane, person”. Our method ensures that new text prompts include both general information and the target classes of the original image. This technique helps the synthetic image to have a clear layout similar to the original one and also addresses the problem of missing labeled classes in the synthetic image.

3.2.2 Visual Prior Blending

Unlike Stable Diffusion models that typically only use text prompts to generate images, Controllable

Algorithm 1: Class balancing algorithm for dataset generation

```

Input: Original dataset  $\mathcal{D}_{\text{origin}}$ ; Target
       images per class  $n_{\text{balance}}$ 
Output: Balanced dataset  $\mathcal{D}_{\text{final}}$ 
1 Stage 1: Initialization /* Storing
   images per class */
2  $\mathcal{M} \leftarrow \emptyset$ 
3 for  $I$  in  $\mathcal{D}$  do
4   for  $C$  in  $I$  do
5      $\mathcal{M}[C] \leftarrow \mathcal{M}[C] \cup \{I\}$ 
6 Stage 2: Sorting /* Sorting by number
   of classes */
7 for  $C$  in  $\mathcal{M}$  do
8   Sort  $\mathcal{M}[C]$ 
9 Stage 3: Balancing /* Generating
   additional images */
10  $\mathcal{D}_{\text{gen}} \leftarrow \emptyset$ 
11 for  $C$  in  $\mathcal{M}$  do
12   while  $\text{len}(\mathcal{M}[C]) < n_{\text{balance}}$  do
13     for  $I$  in  $\mathcal{M}[C]$  do
14       Generate  $I_{\text{gen}}$  based on  $I$ 
15        $\mathcal{M}[C] \leftarrow \mathcal{M}[C] \cup \{I_{\text{gen}}\}$ 
16        $\mathcal{D}_{\text{gen}} \leftarrow \mathcal{D}_{\text{gen}} \cup \{I_{\text{gen}}\}$ 
17     if  $\text{len}(\mathcal{M}[C]) \geq n_{\text{balance}}$  then
18       break
19  $\mathcal{D}_{\text{final}} \leftarrow \mathcal{D}_{\text{gen}} \cup \mathcal{D}_{\text{origin}}$ 
20 return  $\mathcal{D}_{\text{final}}$ 

```

Generation models require additional input guidance (Canny Edge (Canny, 1986), Sketch-Guided (Su et al., 2021), Line-Art Edge (Chan et al., 2022), Depth Map (Ranftl et al., 2022), HED soft edge (Xie and Tu, 2015)) generated from the visual prior detector to determine the image layout. Canny, Line-Art Edge, and Sketch are the visual priors we propose using to balance the diversity of the image and the precise structure of the generated classes in the image. Our default visual prior is Line-Art Edge to generate visual guidance. In Section 4.3.5, we also discuss other types of visual priors to see how effectively they augment the data. Using the T2I-Adapter (Mou et al., 2023) model, the Line Art Detector converts the image into visual prior in-line drawings for each input image. Then, the Adapter generates different resolution features, performing conditional operations at each time step with the UNet denoiser’s features.

In general, methods such as Line-Art Edge, Canny Edge, or HED soft edge all suffer from the limitation that the labeled classes in the image may be blurred or small in size, leading to inaccuracies in describing

Table 1: **Semantic Segmentation Evaluation:** Comparison in mIoU (%) on val set between models’ training on the original training set (D_{origin}) and the extended training set (D_{final}).

Dataset	VOC7			VOC12			
Number images		209	92	183	366	732	1464
DeepLabV3+ Resnet50	D_{origin}	46.54	29.91	38.21	49.40	58.20	61.84
	$D_{gen} \cup D_{origin}$	50.27	33.87	41.45	52.22	60.11	63.06
	Δ	$\uparrow 3.73$	$\uparrow 3.96$	$\uparrow 3.24$	$\uparrow 2.78$	$\uparrow 1.91$	$\uparrow 1.22$
PSPNet Resnet50	D_{origin}	47.04	31.87	38.96	46.62	57.48	62.39
	$D_{gen} \cup D_{origin}$	50.01	34.67	41.46	49.34	61.09	63.78
	Δ	$\uparrow 2.97$	$\uparrow 2.80$	$\uparrow 2.50$	$\uparrow 2.72$	$\uparrow 3.61$	$\uparrow 1.39$
Mask2Former Resnet50	D_{origin}	48.28	34.85	39.63	51.37	59.94	63.65
	$D_{gen} \cup D_{origin}$	49.69	35.53	40.29	51.77	60.02	62.56
	Δ	$\uparrow 1.41$	$\uparrow 0.68$	$\uparrow 0.66$	$\uparrow 0.40$	$\uparrow 0.08$	$\downarrow 1.09$

the structure of the labeled classes within the conditional image. Figure 4a shows an image produced using Line Art Detection. However, the edge results in this case are missing some details of the person, and the TV monitor is almost absent. The red shapes indicate the missing details in the image. This loss of information also occurs when using HED or Canny Edge. These weaknesses result in mislabeling in the synthetic image compared to the original image. We observed that although the segmentation labels of real images cannot fully describe an image’s content, they provide accurate information about the labeled classes. Based on this observation, we propose combining the real image’s prior visualization with the labels before feeding them into the controlled image generation model. The combination of the prior visual image $I_i(\mathcal{V}_i^I)$ and prior visual segmentation label $\mathcal{S}_i(\mathcal{V}_i^S)$ ensures that the generated image has a clear layout and well preserves structures the class labeled information. Our proposed combines \mathcal{V}_i^I and \mathcal{V}_i^S by a weighted sum:

$$\mathcal{V}_i^* = \omega_1 \mathcal{V}_i^I + \omega_2 \mathcal{V}_i^S \quad (4)$$

With ω_1, ω_2 being the trade-off scales when combining \mathcal{V}_i^I and \mathcal{V}_i^S . This combination results in a prior visual that is clear in content and complete information about labeled classes. Figure 4b shows how the Visual Prior Blending method can preserve the structure labeled classes in an image.

3.3 Create class-balancing dataset

To address the issue of class imbalance during model training, we aim for the final dataset D_{final} , which merges the original dataset D_{origin} and the synthetic dataset D_{gen} , to have a balanced distribution among

classes. To create a balanced dataset from the original dataset D_{origin} , we use the class balancing algorithm to generate the dataset D_{gen} based on the balancing factor $n_{balance}$, as presented in Algorithm 1. The algorithm consists of three main stages: Initialization, Sorting, and Balancing. In Stage 1, a dictionary \mathcal{M} is initialized to map each class to its associated images. Each image I is linked to a list of classes it contains. In the next stage, images are arranged in ascending order based on the number of classes they represent, prioritizing those with fewer classes to be generated to maintain the balance. In the final stage, additional images are generated for each class until they reach $n_{balance}$, ensuring an even distribution among classes. This process ensures the dataset is balanced, preventing the overrepresentation of any class and promoting more robust model training.

After generating high-quality training samples, the synthetic dataset D_{gen} and the original dataset D_{origin} are merged into an extended dataset D_{final} for training:

$$D_{final} = D_{gen} \cup D_{origin} \quad (5)$$

In the default setting, we choose an appropriate $n_{balance}$ such that $|D_{gen}| \approx |D_{origin}|$ where $|\cdot|$ is the number of images in the dataset. In Section 4.3.2, we further discuss the impact of varying the number of generated synthetic images.

Table 2: Evaluation results of the DeepLabV3+ model on the PASCAL VOC7 dataset trained on D_{origin} and D_{final} .

D_{origin}	89.32	75.35	43.90	53.95	38.03	51.72	50.81	67.41	72.0	7.77	24.61
D_{final}	88.69	67.67	45.35	57.00	38.07	56.08	70.14	70.67	73.46	28.81	45.45
											mIoU (%)
D_{origin}	41.67	45.16	42.29	66.08	72.71	42.00	14.07	24.68	40.74	12.96	46.54
D_{final}	39.48	36.27	50.10	55.80	71.49	40.29	21.91	18.10	48.13	32.72	50.27

4 RESULTS

4.1 Experiment Details

4.1.1 Dataset

In this section, we evaluate our method on the segmentation datasets VOC7 and VOC12 (Everingham et al., 2015). PASCAL VOC 2007 has 422 images annotated for semantic segmentation, split into 209 training and 213 validation images. Meanwhile, VOC12 has training and validation sets, including 1,464 and 1,449 images. In addition to training on the entire VOC12 dataset (1,464 images), we also train our model using 1/2 (732 images), 1/4 (366 images), 1/8 (183 images), and 1/16 (92 images) partition protocols (Wang et al., 2022). These evaluations on smaller subsets demonstrate the effectiveness of our method in real-world, limited-data scenarios.

4.1.2 Implementation details

We construct our framework on the deep learning PyTorch framework (Paszke et al., 2019) and T2I-Adapter (Mou et al., 2023) using Stable Diffusion XL 1.0 (Podell et al., 2024) with 30 time steps. We generate data using values for ω_1 and ω_2 , as defined in Section 4.3. For semantic segmentation, we employ the DeepLabV3+ (Chen et al., 2018), PSPNet (Zhao et al., 2017), and Mask2Former (Cheng et al., 2022) with segmenters implemented in the MMSegmentation framework (MMSegmentation Contributors, 2020). We utilize the SGD optimizer with standard settings in MMSegmentation. We train our models with an input image size of 512×512 with 30k steps on the Pascal VOC datasets, including VOC7 and VOC12. During training, we only apply simple transformation methods to augment data, such as: *RandomResize*, *RandomCrop*, *RandomFlip*. The performance of the trained model on the applied data is assessed using the Mean Intersection over Union (mIoU) metric.

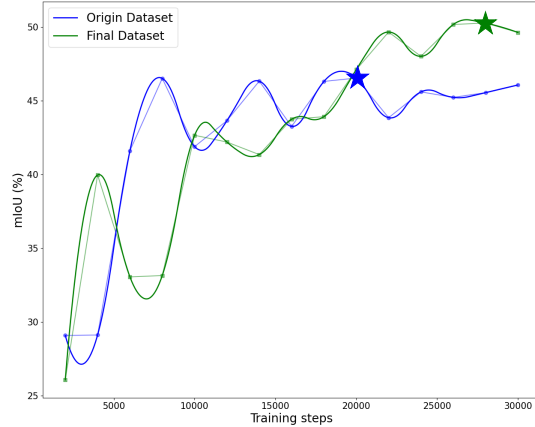


Figure 5: The mIoU (%) of the DeepLabV3+ model over 30k training steps. The star symbol indicates the point of convergence, where the model achieves its highest performance on the validation set.

4.2 Main Results

4.2.1 Quantitative results:

The results presented in Table 1 demonstrate that combining augmented data (D_{gen}) with the original dataset (D_{origin}) improves the performance of various segmentation models on the VOC7 and VOC12 datasets. All models, including DeepLabV3+, PSPNet, and Mask2Former, significantly improve when augmented data. DeepLabV3+ consistently performs the best across different dataset sizes. We note that as the amount of real-world data increases, the accuracy of the generated images and labels becomes crucial. Mismatched generated images in the synthetic data can lead to performance degradation; this is observed in Mask2Former when trained on the VOC12 dataset with 1464 images.

Figure 5 visualizes the validation set accuracy on the PASCAL VOC7 dataset over 30,000 steps using the DeepLabV3+ model. The results show that training the model on the D_{final} achieves 50.27% mIoU, 3.73% higher than training solely on the D_{origin} . The



Figure 6: Some results show the limitations of direct generation and the effectiveness of our method to overcome them.

Table 3: Impact of Class-Prompt Appending (1), Visual Prior Blending (2), Class balancing algorithm (3), and Post Filter (Fang et al., 2024) (4).

(1)	(2)	(3)	(4)	mIoU (%)
				42.15
✓				47.60
	✓			47.25
✓	✓			48.98
✓	✓	✓		50.27
✓	✓	✓	✓	52.23

Table 4: Effect of the number of synthetic data generated on data balance and performance.

n _{gen}	R/S	Entropy ↑	CIR ↓	mIoU (%)
-	209/0	3.944	0.253	46.54
27	209/216	4.044	0.231	50.27
41	209/425	4.042	0.231	50.37
55	209/634	4.059	0.224	49.25
69	209/845	4.057	0.225	47.32

visualization also indicates that the model converges earlier when trained on the D_{origin} compared to the D_{final} . Additionally, the detailed performance for each class in the PASCAL VOC dataset provided in Table 2 demonstrates that most classes show improved accuracy when trained on the D_{final} dataset.

Notably, some classes, such as “bus”, “cow”, “chair”, and “TV monitor”, exhibit significant improvements.

4.2.2 Qualitative results

In Figure 6, each row presents three images: the original image, the image generated by the Controllable Generation model (using prompts generated by BLIP-2), and the image produced by the generation model with our proposed pipeline. For the images generated by the SD model without our method, the first two rows illustrate cases where labeled classes in the image are missing in the generated description, causing the model to fail in accurately generating all those classes. In the third row, the image contains objects belonging to the “cow” class with smaller sizes, which prevents the Image Captioning Model from including “cow” in the description, resulting in an inaccurate generated image without cows. In the last row, although the case is relatively simple and the prompt includes all the labeled classes, the generated image still fails to depict the structure of both “bird” objects accurately. All four images are significantly improved with our proposed pipeline, with the labeled objects entirely generated and their structure well preserved. This demonstrates that our method effectively

Table 5: Performance of different text prompt selections

Method	Example	mIoU (%)
Generated caption	A room with a table and a laptop on it	47.24
Simple text prompt	A photo of sofa, chair, dining table	48.21
Class-Prompt Appending	A room with a table and a laptop on it; sofa, chair, dining table	50.27

Table 6: Study on different trade-off scales

ω_2	ω_1				
	0.6	0.7	0.8	0.9	1.0
0.7	47.12	47.32	46.42	45.36	45.38
0.8	48.51	48.93	48.32	47.09	46.79
0.9	49.13	50.27	49.11	48.79	48.36
1.0	48.13	49.32	48.91	48.33	47.03

addresses the limitations of directly using Controllable Image Generation models.

4.3 Ablation Study

We conduct all ablation study experiments using the DeepLabV3+ model, backbone Resnet50 with training and evaluation details described in Section 4.1.2. The model is trained on the PASCAL VOC7 dataset, and the results are evaluated on the val set.

4.3.1 Effects of different methods:

The performance of the proposed methods is summarized in Table 4.3.1. When using the Baseline with generated prompts, the performance is only as low as 42.15% mIoU, which is lower than when training on the original data. This demonstrates the essential nature of the proposed methods when generating synthetic data. Our method yields a 50.27% mIoU, showing its effectiveness. Additionally, we experimented with combining the Post Filter with the Category-Calibrated CLIP Rank (Fang et al., 2024) for generating synthetic data. The result of this combination is higher, which shows that our method can combine filters from previous studies (Fang et al., 2024; Wu et al., 2024) to improve the performance.

4.3.2 Effect of number of synthetic data:

The results of the proposed method’s experiments with different amounts of generated synthetic data are summarized in Table 4, R/S refers to the number of real/synthetic images. The metrics we use to evaluate data imbalance include Entropy, and Class Imbalance

Ratio (CIR). Initially, without using synthetic data, the model achieves an mIoU of 46.54. When training with synthetic data in quantities of approximately $|D_{origin}|$, $2 \times |D_{origin}|$, and $3 \times |D_{origin}|$, the data balance metrics stabilize at a better level, and model performance improves. However, we observed that using synthetic data around $3 \times |D_{origin}|$ negatively impacts performance, resulting in a decrease compared to training with $1 \times |D_{origin}|$ and $2 \times |D_{origin}|$ of synthetic data.

4.3.3 Text prompt selection:

Table 5 compares different text prompt selection methods for generative modeling. We compare the performance of three prompt types: *Generated caption* generated from the Image Captioning model, *Simple text prompt* listing the classes in the image, and *Class-Prompt Appending*, a combination of the two prompt types. *Class-Prompt Appending* outperforms the other two methods by 50.27 mIoU (%), precisely 3.03 and 2.06 better than *generated caption* and *simple text prompt*, respectively, in mIoU. These results show that the *Class-Prompt Appending* text prompt selection method can support SD in generating diverse datasets and ensuring accurate attention.

4.3.4 Effect of different trade-off scales:

Trade-off scales are utilized to combine the visual prior of the image with the semantic segmentation map presented in Section 3.2.2. We tested various scales and documented the results in Table 4.3.4. The outcomes indicate that the scale $\omega_1=0.7$ and $\omega_2=0.9$ yields the best results, with ω_2 enabling proper localization of the labeled classes. On the other hand, the scale $\omega_1=0.7$ retains the general content of the image without needing to be as detailed as the original image.

4.3.5 Other Visual Priors

We compare using different visual priors for both T2I-Adapter (Mou et al., 2023) and ControlNet (Zhang



Caption: Caption a room with a table and a laptop on it

Class labels: sofa, chair, dining table

Figure 7: Some image generation results from various Controllable models when combined with our proposed approach.

Table 7: Different visual priors controlled the enhancement results. All used the Stable Diffusion XL version.

	T2I-Adapter			ControlNet	Inpainting
	LineArt	Canny	Sketch	Canny	
mIoU (%)	50.27	48.95	47.52	48.95	47.56

et al., 2023): Line Art (Chan et al., 2022), Canny (Canny, 1986), Sketch (Su et al., 2021). We also combine Inpainting (Rombach et al., 2022) with our methods (excluding Visual Prior Blending). Although the T2I-Adapter combined with Line Art gives the best result at 50.27% mIoU, other visual priors also show competitive performance, especially Canny on both T2I-Adapter and ControlNet. Figure 7 shows some image results with Controllable Diffusion model.

5 DISCUSSION AND CONCLUSION

5.1 Limitations

While our approach effectively generates synthetic images to augment data for semantic segmentation, there are certain limitations to consider. First, the results in Tables 1, 4 show that the model’s performance may decrease when the number of synthetic images is large or more significant than the number of original real images. This may be because the synthetic images do not completely guarantee the original images’ location and quantity of labels. Additionally, as the images produced by the Stable Diffusion (Podell et al., 2024) model are trained on the LION-5B dataset (Schuhmann et al., 2022), the resulting images do not share the same distribution as the target dataset. So, the synthetic data cannot completely replace the original training dataset used to train the model.

5.2 Conclusion

We introduce a data augmentation pipeline based on a Controllable Diffusion model for semantic segmentation tasks. Our evaluations were performed on the PASCAL VOC dataset, and the results show that our pipeline significantly improves the performance of semantic segmentation models. We note that our method can be combined with other data augmentation methods to enhance performance further. This advancement paves the way for future research in data augmentation using generative models.

REFERENCES

- Azizi, S., Kornblith, S., Saharia, C., Norouzi, M., and Fleet, D. J. (2023). Synthetic data from diffusion models improves imagenet classification. *Transactions on Machine Learning Research*.
- Canny, J. (1986). A computational approach to edge detection. *IEEE Transactions on Pattern Analysis and Machine Intelligence*, PAMI-8(6):679–698.
- Chae, J., Cho, H., Go, S., Choi, K., and Uh, Y. (2023). Semantic image synthesis with unconditional generator. In *Thirty-seventh Conference on Neural Information Processing Systems*.
- Chan, C., Durand, F., and Isola, P. (2022). Learning to generate line drawings that convey geometry and semantics. In *2022 IEEE/CVF Conference on Computer Vision and Pattern Recognition (CVPR)*, pages 7905–7915.
- Chen, L.-C., Zhu, Y., Papandreou, G., Schroff, F., and Adam, H. (2018). Encoder-decoder with atrous sepa-

- rable convolution for semantic image segmentation. In Ferrari, V., Hebert, M., Sminchisescu, C., and Weiss, Y., editors, *Computer Vision – ECCV 2018*, pages 833–851, Cham.
- Cheng, B., Misra, I., Schwing, A. G., Kirillov, A., and Girdhar, R. (2022). Masked-attention mask transformer for universal image segmentation. In *2022 IEEE/CVF Conference on Computer Vision and Pattern Recognition (CVPR)*.
- Everingham, M., Eslami, S. M. A., Gool, L. V., Williams, C. K. I., Winn, J., and Zisserman, A. (2015). The pascal visual object classes challenge: A retrospective. *International Journal of Computer Vision*, 111(1):98–136.
- Fang, H., Han, B., Zhang, S., Zhou, S., Hu, C., and Ye, W.-M. (2024). Data augmentation for object detection via controllable diffusion models. In *2024 IEEE/CVF Winter Conference on Applications of Computer Vision (WACV)*, pages 1246–1255.
- He, R., Sun, S., Yu, X., Xue, C., Zhang, W., Torr, P., Bai, S., and Qi, X. (2023). IS SYNTHETIC DATA FROM GENERATIVE MODELS READY FOR IMAGE RECOGNITION? In *The Eleventh International Conference on Learning Representations*.
- Ho, J., Jain, A., and Abbeel, P. (2020). Denoising diffusion probabilistic models. In *Advances in Neural Information Processing Systems*, volume 33, pages 6840–6851.
- Li, J., Li, D., Savarese, S., and Hoi, S. (2023). Blip-2: bootstrapping language-image pre-training with frozen image encoders and large language models. In *Proceedings of the 40th International Conference on Machine Learning, ICML’23*.
- Lin, T.-Y., Maire, M., Belongie, S., Hays, J., Perona, P., Ramanan, D., Dollár, P., and Zitnick, C. L. (2014). Microsoft coco: Common objects in context. In *Computer Vision – ECCV 2014*, pages 740–755, Cham. Springer International Publishing.
- MMSegmentation Contributors (2020). OpenMMLab Semantic Segmentation Toolbox and Benchmark.
- Mou, C., Wang, X., Xie, L., Wu, Y., Zhang, J., Qi, Z., Shan, Y., and Qie, X. (2023). T2i-adapter: Learning adapters to dig out more controllable ability for text-to-image diffusion models.
- Nguyen, Q. H., Vu, T. T., Tran, A. T., and Nguyen, K. (2023). Dataset diffusion: Diffusion-based synthetic data generation for pixel-level semantic segmentation. In *Thirty-seventh Conference on Neural Information Processing Systems*.
- Paszke, A., Gross, S., Massa, F., Lerer, A., Bradbury, J., Chanan, G., Killeen, T., Lin, Z., Gimelshein, N., Antiga, L., Desmaison, A., Kopf, A., Yang, E., DeVito, Z., Raison, M., Tejani, A., Chilamkurthy, S., Steiner, B., Fang, L., Bai, J., and Chintala, S. (2019). Pytorch: An imperative style, high-performance deep learning library. In *Advances in Neural Information Processing Systems*, volume 32.
- Podell, D., English, Z., Lacey, K., Blattmann, A., Dockhorn, T., Müller, J., Penna, J., and Rombach, R. (2024). Sdxl: Improving latent diffusion models for high-resolution image synthesis. In *The Twelfth International Conference on Learning Representations*.
- Ranftl, R., Lasinger, K., Hafner, D., Schindler, K., and Koltun, V. (2022). Towards robust monocular depth estimation: Mixing datasets for zero-shot cross-dataset transfer. *IEEE Transactions on Pattern Analysis and Machine Intelligence*, 44(3).
- Rombach, R., Blattmann, A., Lorenz, D., Esser, P., and Ommer, B. (2022). High-resolution image synthesis with latent diffusion models. In *Proceedings of the IEEE/CVF Conference on Computer Vision and Pattern Recognition (CVPR)*, pages 10684–10695.
- Schuhmann, C., Beaumont, R., Vencu, R., Gordon, C. W., Wightman, R., Cherti, M., Coombes, T., Katta, A., Mullis, C., Wortsman, M., Schramowski, P., Kundurthy, S. R., Crowson, K., Schmidt, L., Kaczmarczyk, R., and Jitsev, J. (2022). LAION-5b: An open large-scale dataset for training next generation image-text models. In *Thirty-sixth Conference on Neural Information Processing Systems Datasets and Benchmarks Track*.
- Su, Z., Liu, W., Yu, Z., Hu, D., Liao, Q., Tian, Q., Pietikäinen, M., and Liu, L. (2021). Pixel difference networks for efficient edge detection. In *2021 IEEE/CVF International Conference on Computer Vision (ICCV)*, pages 5097–5107.
- Trabucco, B., Doherty, K., Gurinas, M. A., and Salakhutdinov, R. (2024). Effective data augmentation with diffusion models. In *The Twelfth International Conference on Learning Representations*.
- Wang, Y., Wang, H., Shen, Y., Fei, J., Li, W., Jin, G., Wu, L., Zhao, R., and Le, X. (2022). Semi-supervised semantic segmentation using unreliable pseudo labels. In *Proceedings of the IEEE/CVF International Conference on Computer Vision and Pattern Recognition (CVPR)*.
- Wu, W., Dai, T., Huang, X., Ma, F., and Xiao, J. (2024). Gpt-prompt controlled diffusion for weakly-supervised semantic segmentation.
- Xie, S. and Tu, Z. (2015). Holistically-nested edge detection. In *2015 IEEE International Conference on Computer Vision (ICCV)*, pages 1395–1403.
- Yu, F., Chen, H., Wang, X., Xian, W., Chen, Y., Liu, F., Madhavan, V., and Darrell, T. (2020). Bdd100k: A diverse driving dataset for heterogeneous multitask learning. In *IEEE/CVF Conference on Computer Vision and Pattern Recognition (CVPR)*.
- Zhang, L., Rao, A., and Agrawala, M. (2023). Adding conditional control to text-to-image diffusion models. In *2023 IEEE/CVF International Conference on Computer Vision (ICCV)*, pages 3813–3824.
- Zhao, H., Shi, J., Qi, X., Wang, X., and Jia, J. (2017). Pyramid scene parsing network. In *Proceedings of the IEEE Conference on Computer Vision and Pattern Recognition (CVPR)*.
- Zhou, B., Zhao, H., Puig, X., Xiao, T., Fidler, S., Barriuso, A., and Torralba, A. (2019). Semantic understanding of scenes through the ade20k dataset. *International Journal of Computer Vision*, 127(3):302–321.